*Journal of Non-Newtonian Fluid Mechanics*, 44 (1992) 15–36
Elsevier Science Publishers B.V., Amsterdam



# Interrelation between continuous and discrete relaxation time spectra

M. Baumgaertel and H.H. Winter

*University of Massachusetts at Amherst, Department of Chemical Engineering, Amherst, MA 01003 (USA)*

(Received October 14, 1991)

## Abstract

A relation has been derived between the continuous and the discrete forms of linear viscoelastic relaxation-time spectra. Both forms can be interconverted, and they are equivalent in their ability to reproduce $G'(\omega)$, $G''(\omega)$, or $G(t)$ data. The linear superposition of even only a few Maxwell-modes is able to mimic the continuous form. This rapid conversion leads to the 'parsimonious' spectrum which models the linear viscoelastic relaxation with the smallest possible number of modes. Typical experimental spectra of broadly distributed and of monodisperse polymers provide the means for testing the proposed relations. Effects of noise and data density were studied for $G'$, $G''$-data sets.

*Keywords:* relaxation time spectrum; Maxwell-mode; parsimonious spectrum; BSW-spectrum

## 1. Introduction

The molecular mobility of polymeric liquids and solids expresses itself in a relaxation-time spectrum. This can be seen when mechanically probing the material over a wide range of time scales or rates. The relaxation-time

*Correspondence to*: H.H. Winter, Dept. of Chemical Engineering, University of Massachusetts, Amherst, MA 01003, USA.

0377-0257/92/$05.00 © 1992 – Elsevier Science Publishers B.V. All rights reserved

spectrum, denoted as 'spectrum' in the following, may be written as a continuous function, $H(\lambda)$, or as a sum of discrete terms, each of them having a characteristic time constant, $\lambda_i$. The best known molecular models for the relaxation of linear macromolecules predict discrete spectra in which the individual relaxation modes are prescribed by molecular parameters of the polymer [1–3]. Experimentalists are also used to determine discrete spectra from their linear viscoelastic experiments. Discrete spectra are also used extensively in flow modeling. They have the advantage that they can easily be integrated for predicting a wide range of linear viscoelastic material functions [4]. Even if one knows the continuous function $H(\lambda)$ for a specific material, one may want to convert it into its discrete form for easier calculations of these viscoelastic material functions.

The relaxation-time spectrum of viscoelastic materials, $H(\lambda)$, is commonly defined through measurable linear viscoelastic material functions such as the relaxation modulus $G(t)$ [4]

$$G(t) = G_e + \int_0^\infty H(\lambda) \exp(-t/\lambda) \frac{d\lambda}{\lambda} \tag{1}$$

with an equilibrium modulus $G_e$ which is finite for viscoelastic solids and zero for viscoelastic liquids. The spectrum is also the kernel of several important rheological functions like the storage modulus, $G'(\omega)$, and the loss modulus $G''(\omega)$

$$G'(\omega) = G_e + \int_0^\infty H(\lambda) \frac{\omega^2\lambda^2}{1+\omega^2\lambda^2} \frac{d\lambda}{\lambda}, \tag{2}$$

$$G''(\omega) = \int_0^\infty H(\lambda) \frac{\omega\lambda}{1+\omega^2\lambda^2} \frac{d\lambda}{\lambda}. \tag{3}$$

There is an infinite number of ways for discretizing a specific continuous spectrum. We therefore have to make a few choices before we continue. Discrete relaxation modes, for instance, may be expressed by very different choices of decaying time functions. Examples are exponential decays or Maxwell-modes [5], stretched exponentials or Kohlrausch-modes [6], truncated power laws or BSW-modes [7]. Differences between these modes are insignificant for infinitely close spacings of the relaxation times, however, they become important with wider spacings. Maxwell-modes, $g_i$, $\lambda_i$, $i = 0, 1, 2, \ldots, N$, have been preferred since they are most easily incorporated in modeling calculations. The relaxation modulus, for instance, becomes

$$G(t) = G_e + \sum_{i=0}^{N} g_i \exp(-t/\lambda_i). \tag{4}$$

The corresponding relaxation time spectrum may be expressed as

$$H(\lambda) = \sum_{i=0}^{N} g_i \, \delta\left(1 - \frac{\lambda}{\lambda_i}\right), \tag{5}$$

where $\delta(x)$ denotes the Dirac delta function which has unit area and zero value everywhere except at $x = 0$ where its value is 1. The following discretization will be restricted to such Maxwell modes.

The relaxation spectrum $H(\lambda)$ cannot be measured directly in an experiment. In practice, linear viscoelastic data such as the dynamic moduli $G'(\omega)$, $G''(\omega)$, the dynamic compliance $J'(\omega)$, $J''(\omega)$, the relaxation modulus $G(t)$, or the creep compliance $J(t)$ are directly converted into $H(\lambda)$ by means of heuristic formulae [8] or the data are suitably fitted by discrete spectra. Such fitting methods include least-square approximations [9–11], Contin [12], regularization methods [13,14] and maximum entropy methods [15,16]. Some of the methods have been compared recently by Orbey and Dealy [17]. Baumgaertel and Winter [11] recently proposed a method for representing the relaxation spectrum of a material with the fewest possible Maxwell-modes while remaining within the experimental scatter of the available $G'$, $G''(\omega)$ data. Such a representation is called a 'parsimonious' model (PM-spectrum). It is based on the idea that the discrete relaxation times should be freely adjustable so that they converge to values which are characteristic for the material. Neighboring relaxation modes are allowed to merge so that the number of modes gradually shrinks until the PM-spectrum model is found. The spacings between neighboring modes depend on the specific material. A major advantage of the parsimonious model is the rapid conversion of the regression algorithm, even for very complicated spectra. The regression procedure is assigned to a standard software called IRIS and, for brevity, we shall identify the calculated spectra as PM-spectra having PM-modes and PM-standard deviations in their ability to fit data. Throughout this paper, PM-modes will be calculated and used as a convenient way of describing $G'$, $G''$ data. This gradually will lead to an understanding of the parsimonious model.

The determination of discrete spectra is understood quite well; however, it seems to be difficult to convert these spectra into continuous ones and vice versa. This will be addressed in the following study. As a starting point, we postulate that there always exists a discrete set of Maxwell-modes which represents the continuous spectrum with sufficient accuracy, even if the spacing between two neighboring relaxation times may be fairly large. The consequences of such discretization have to be explored in greater detail. For that purpose, we choose two typical continuous spectra, $H(\lambda)$, and express them with a sum of representative Maxwell-modes. By increasing

the spacing between neighboring relaxation times, we attempt to find the 'parsimonious' spectrum which represents the continuous spectrum with the fewest possible discrete modes. Necessary criteria will be defined for distinguishing an acceptable spectrum from an unacceptable one.

## 2. Interrelation between continuous and discrete relaxation-time spectra

For the discretization of the continuous spectrum $H(\lambda)$, one may lump sections of $H(\lambda)$ within time windows $[\lambda_i^+ \ldots \lambda_i^-]$ around $\lambda_i$ into representative Maxwell-modes. This is sketched in Fig. 1. The relation between the Maxwell-modes and the continuous spectrum will be analyzed in the following. In our analysis we start out with a set of discrete relaxation times, $\lambda_i$, $i = 0, 1, 2, \ldots, N$. The spacing

$$\frac{\lambda_i}{\lambda_{i+1}} = a_i, \text{ with } \lambda_i > \lambda_{i+1} \text{ (therefore } a > 1) \tag{6}$$

can be chosen to be either equidistant or non-equidistant on a logarithmic time scale. In the case of equidistant spacing, all spacing factors $a_i$ are identical ($a_i = a$). Following the usual convention, the zeroth mode has the longest relaxation time and the $\lambda_i$ values decrease monotonically with increasing $i$.

For the window boundaries, $\lambda_i^+$ and $\lambda_i^-$, one may choose geometric averages of the relaxation time $\lambda_i$ and its neighboring relaxation times $\lambda_{i+1}$ and $\lambda_{i-1}$, respectively

$$\lambda_i^+ = \sqrt{\lambda_i \lambda_{i+1}} \text{ and } \lambda_i^- = \sqrt{\lambda_i \lambda_{i-1}}\,. \tag{7}$$

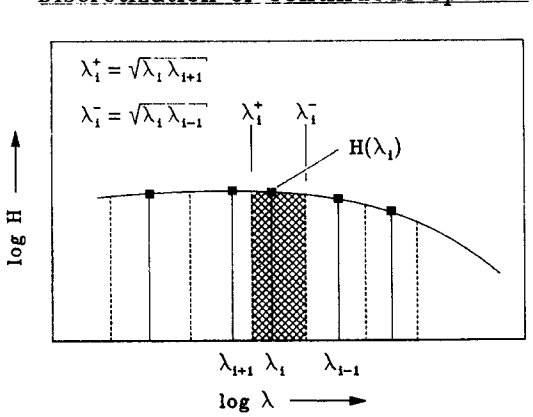


Fig. 1. Schematic of the discretization of a continuous spectrum. Sections of the continuous spectrum $[\lambda_i^+ \ldots \lambda_i^-]$ are lumped into discrete relaxation modes.

This specific choice gives acceptable results as will be shown below.

The relaxation strength, $g_i$, is obtained by integration of $H(\lambda)$ in this finite relaxation time window, $[\lambda_i^+ \ldots \lambda_i^-]$. Comparison of eqns. (1) and (4) shows that the $i$th representative Maxwell-mode is given as

$$g_i \exp(-t/\lambda_i) = \int_{\lambda_i^+}^{\lambda_i^-} H(\lambda) \exp(-t/\lambda) \frac{d\lambda}{\lambda} \text{ with } t > 0. \tag{8}$$

For a narrow spacing of the relaxation times eqn. (8) simplifies to

$$g_i = \ln \sqrt{\lambda_{i-1}/\lambda_{i+1}}\, H(\lambda_i). \tag{9}$$

This relationship simplifies even further for a narrow equidistant spacing

$$g_i = \ln a\, H(\lambda_i). \tag{10}$$

Note that the relaxation modes fall onto the continuous spectrum $g_i = H(\lambda_i)$ for the special case $\ln a = 1$ or $a = 2.72$.

The discrete spectrum converges to the continuous spectrum for the limiting case that the spacing is very close ($a \to 1$). It will be interesting to find out how far apart the modes can be spaced without violating the above eqns. (9) and (10).

In the next Section two typical continuous spectra, one for broadly distributed linear polymers and one for narrowly distributed linear polymers, are discretized using eqn. (10). Discretization artifacts are demonstrated on related material functions such as $G'(\omega)$, $G''(\omega)$, $G(t)$. Utilizing eqn. (9), we shall also show that discrete PM-spectra [11] have an equivalent continuous form. Consistency tests confirm the conversion procedure.

## 3. Case studies: Discretization

### *3.1 Discretizing 'smooth' relaxation-time spectra*

In the first case study we discretize a smooth spectrum which has no sudden jumps or cut-offs. This type of spectrum is often observed for broadly distributed linear flexible polymers. Examples are data of three broadly distributed polypropylenes with different molar masses [18]. The dynamic data $G'$, $G''$ of these samples are shown in Fig. 2. The dashed lines represent the fit of the data using discrete PM-spectra. Surprisingly, we find that a continuous BSW-spectrum [7] with a stretched exponential cut-off at a characteristic relaxation time $\lambda'_{max}$

$$H(\lambda) = \left[ n_e G_N^0 \left( \frac{\lambda}{\lambda_e} \right)^{n_e} + H_g \left( \frac{\lambda}{\lambda_e} \right)^{n_g} \right] \exp(-\lambda/\lambda'_{max})^{\beta} \qquad \text{for } M_w \gg M_e \tag{11}$$

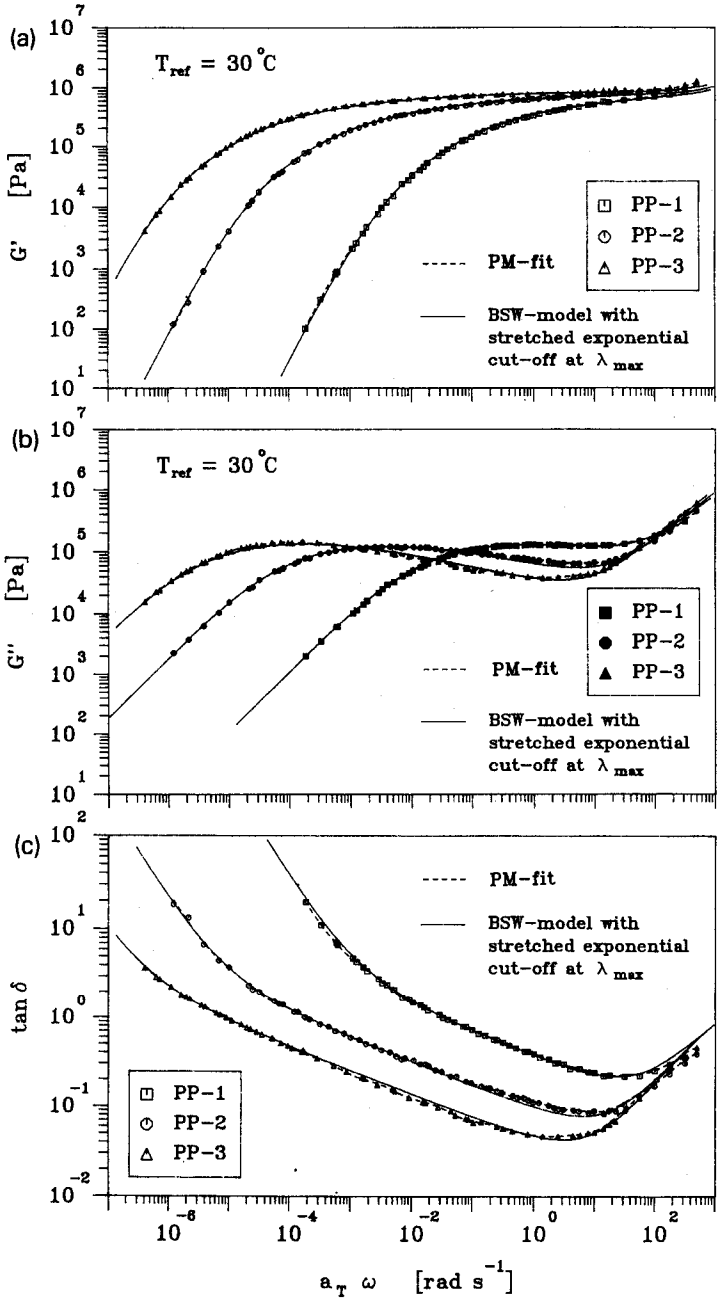


Fig. 2. Storage modulus $G'$ (a), loss modulus $G''$ (b) and loss tangent tan $\delta$ (c) of three broadly distributed polypropylene samples of ref. 18. The molar masses of the samples are PP-1: $M_w = 75000$ g mol$^{-1}$; PP-2: $M_w = 132000$ g mol$^{-1}$ and PP-3: $M_w = 375000$ g mol$^{-1}$ (determined from intrinsic viscosity measurements). The dashed lines represent the fit with the PM-spectrum while the solid lines are calculated with the BSW-model with stretched exponential cut-off at $\lambda'_{max}$ and $\beta = 0.39$.

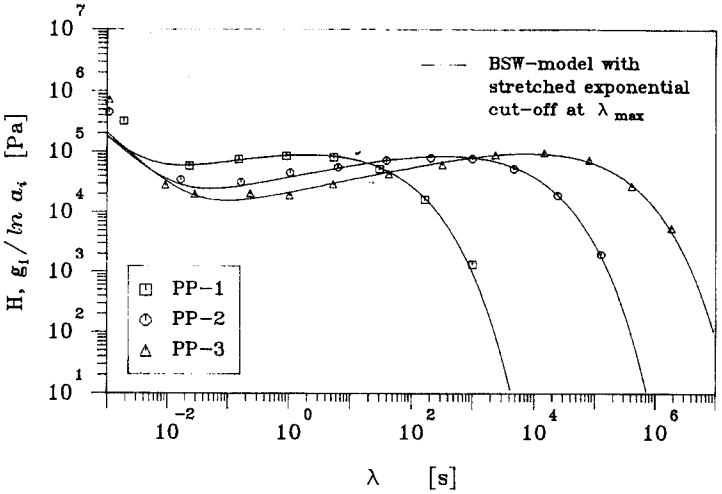


Fig. 3. Relaxation spectra of the samples from Fig. 2. The discrete PM-spectra agree very well with the continuous spectrum.

represents the data extremely well (solid lines in Fig. 2). In this empirical model $G_N^0$ is the plateau modulus, $n_e$ and $n_g$ are the slopes of the spectrum in the entanglement and glass transition regimes, $H_g$ is the glass-transition constant, $\lambda_e$ the relaxation time corresponding to polymer chains with entanglement molar mass. The exponent $\beta$ controls the sharpness of the cut-off of the spectrum. Note that a physical interpretation of this empirical spectrum is not attempted here. This spectrum is identical to a BSW-spectrum for narrowly distributed polymers [7], except for the cut-off at the longest relaxation time $\lambda_{max}$ which is now replaced by a 'soft' stretched exponential cut-off. Using eqn. (9) we find, that within the experimental scatter, the relaxation modes of the parsimonious model (PM-modes) fall onto the continuous BSW-spectrum with stretched exponential cut-off (see Fig. 3). We therefore propose to use eqn. (11) as the spectrum for describing broadly distributed polymers.

Motivated by these experimental findings, we consider the above spectrum as a convenient example which allows testing of the discretization procedure. The results, however, are not limited to this particular type of spectrum. The solid curve in Fig. 4 shows a typical BSW-spectrum with stretched exponential cut-off with an exponent of $\beta = 0.5$. This continuous spectrum is discretized (eqn. (10)) using five different spacings. As expected, the $g_i$-values of the discrete spectra do not fall onto the curve of $H(\lambda)$. Note that all discrete spectra have the same shape. They can actually be generated by shifting the continuous spectrum vertically by an amount

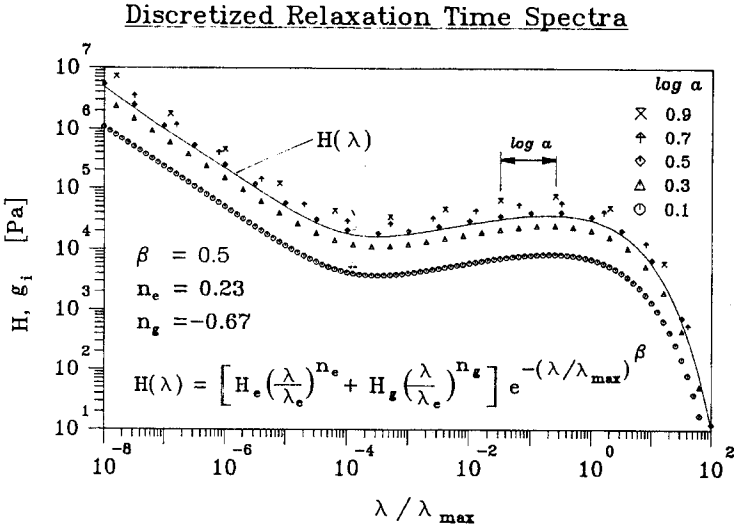


Fig. 4. A typical BSW-spectrum with stretched exponential cut-off ($\beta = 0.5$) at a characteristic relaxation time $\lambda'_{max}$ is discretized. The spacing between neighboring relaxation times is varied from log $a = 0.1$ to 0.9.

ln $a$ (see also eqn. (10) in support of this observation). This is an important observation which seems to be a typical property of discrete spectra. It will be useful in the reverse calculations, i.e. when converting discrete spectra into their continuous form.

Figure 5 shows the dynamic moduli which are calculated from the different forms of the spectrum of Fig. 4. A slight waviness in $G'$ and $G''$, can only be noticed for the spectrum with the widest spacing (log $a = 0.9$). The deviations

$$\Delta' = \log (G'_{dis}/G'_{cont}); \qquad \Delta'' = \log (G''_{dis}/G''_{cont}) \tag{12}$$

show that curves calculated with discrete spectra oscillate around the curves calculated from continuous spectra (Figs. 6(a)–6(b)). The loss modulus $G''$ exhibits a more or less uniform waviness, since the discrete modes contribute locally to this curve, while the storage modulus $G'$ is wavy only near the transition from the terminal zone to the entanglement regime. The peak-to-peak distance of the oscillation is equivalent to the spacing log $a$. The waviness artifact can hardly be recognized if we use 1.5 relaxation times per decade or more.

The calculated relaxation modulus (Fig. 7) is more sensitive to discretization. It becomes wavy in the terminal region if the spacing exceeds log $a = 0.5$. Characteristic steady-state data such as the zero shear viscosity

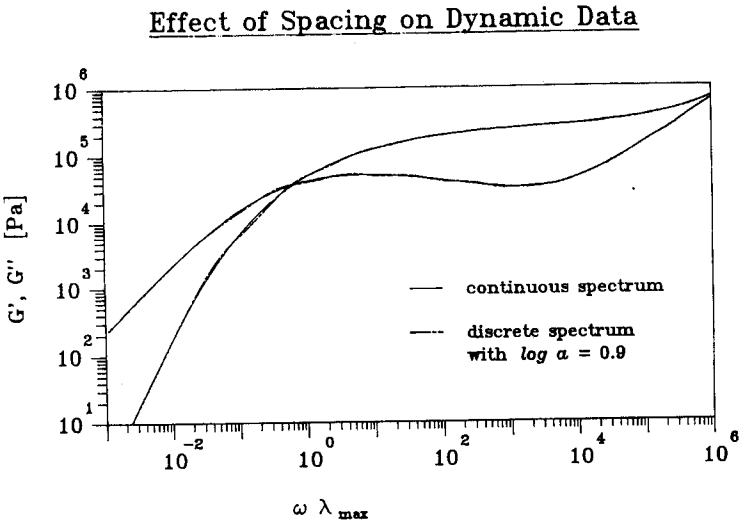


Fig. 5. The dynamic data are calculated from the spectra in Fig. 4. A slight waviness in $G'$ and $G''$ can only be observed if the spacing is very large, $\log a = 0.9$.

$\eta_0$ and the recoverable compliance $J_e^0$ are not noticeably affected by the discretization.

### 3.2 Discretization of relaxation-time spectra with abrupt cut-off

The self-similar relaxation of linear monodisperse polymers is given by a BSW-spectrum with an abrupt cut-off at the longest relaxation time $\lambda_{max}$ [7].

$$H(\lambda) = \begin{cases} n_e G_N^0 \left(\frac{\lambda}{\lambda_{max}}\right)^{n_e} + H_g \left(\frac{\lambda}{\lambda_e}\right)^{-n_g} & \text{for } \lambda < \lambda_{max} \text{ and } M \gg M_c \\ 0 & \text{for } \lambda > \lambda_{max} \end{cases} \quad (13)$$

where $G_N^0$, $n_e$, $H_g$ and $\lambda_e$ are as defined earlier and $\lambda_{max}$ is the longest (cut-off) relaxation time which depends on the 3.4th-power of molar mass. This spectrum will be discretized in the following case study.

Using experimental data, we can demonstrate the parallelism between the continuous and the discrete BSW-spectrum. The dynamic data master curve of a polyisoprene (PIP) standard with a molar mass of $M_w = 305\,000$ g mol$^{-1}$ and polydispersity of 1.05 is shown in Fig. 8. The corresponding BSW-spectrum as shown in Fig. 9 excellently reproduces the dynamic data in Fig. 8. The PM-modes, when divided by ln $a_i$, fall pretty much on the BSW-spectrum. Note that the filled symbols in Fig. 9 represent the discrete

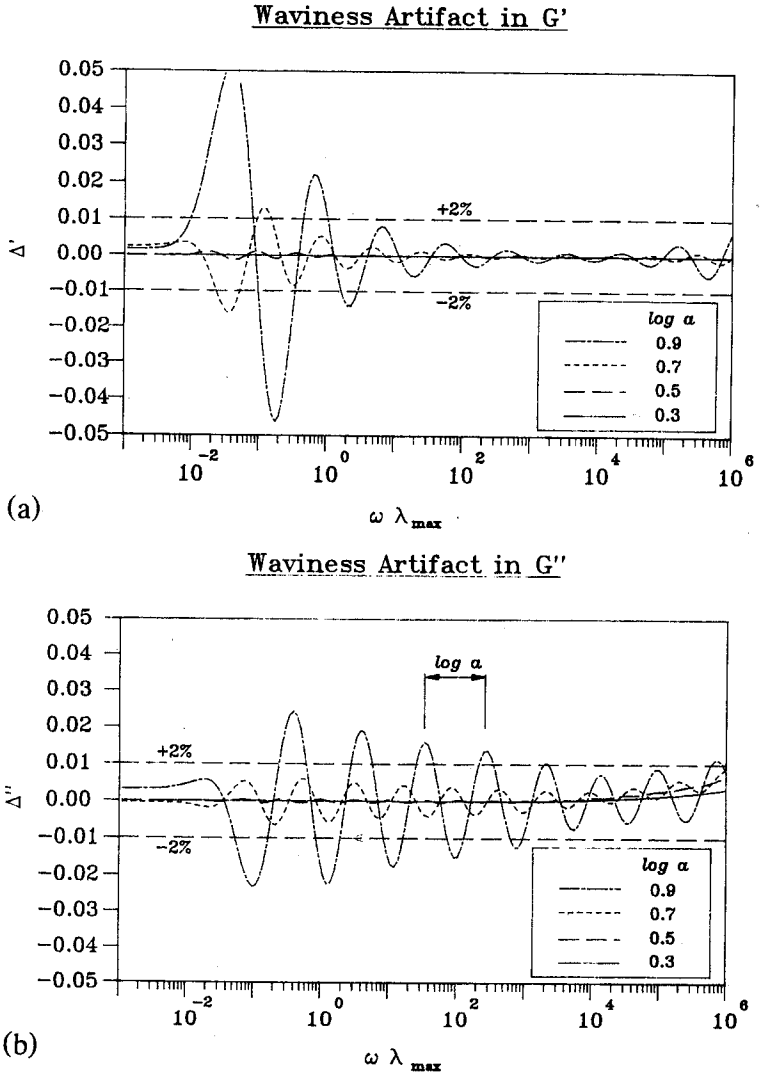


Fig. 6. Deviations between the dynamic data calculated with the discretized spectra and the curve calculated with the continuous spectrum: (a) storage modulus $G'$; (b) loss modulus $G''$.

Maxwell-modes $(g_i, \lambda_i)$ while the unfilled symbols are points on $H(\lambda)$ which are calculated from the Maxwell-modes by dividing the relaxation strength $g_i$ by the local spacing ln $a_i$ (eqn. (9)). The discretization makes the sudden cut-off at $\lambda_{max}$ somewhat more gradual and an additional (weak) Maxwell-mode with a longer relaxation time is needed. This broadening of the spectrum is a discretization artifact which becomes more

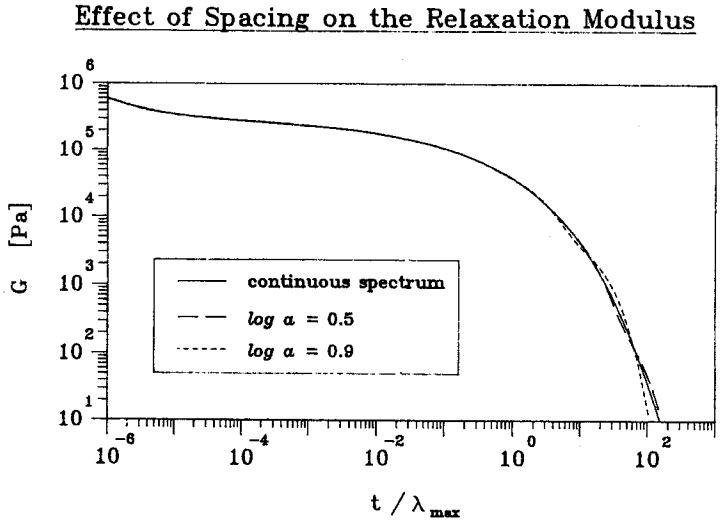


Fig. 7. The relaxation modulus is calculated from the spectra in Fig. 4. The relaxation modulus is insensitive to the spacing of the discrete relaxation times, except for long times where the curves oscillate if the spacing exceeds log $a = 0.5$.

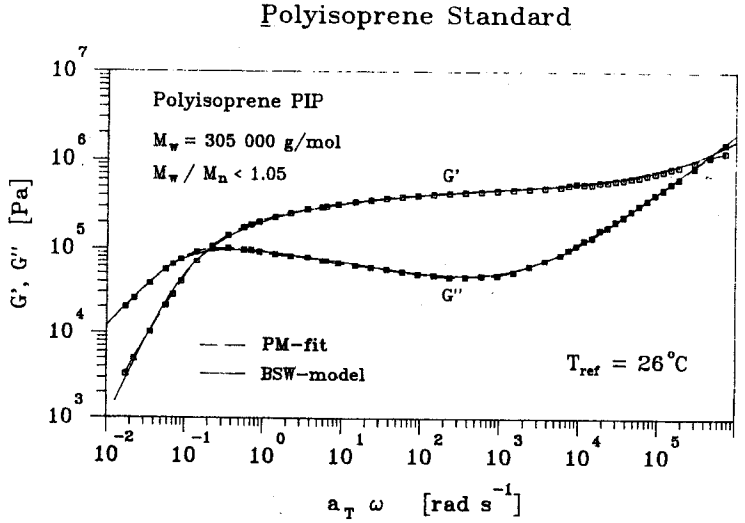


Fig. 8. Dynamic data of a polyisoprene standard synthesized at Polymer Labs. The molar mass of the sample is $M_w = 305\,000$ g mol$^{-1}$ and the polydispersity $M_w/M_w < 1.05$. The solid line through the data points represents the fit of the continuous BSW-spectrum. The dashed line is the fit of the discrete PM-spectrum. The spectrum was measured at several temperatures and then shifted to the reference temperature of 26°C. The rheometer was a Rheometrics RDS 7700 with parallel disk fixtures.

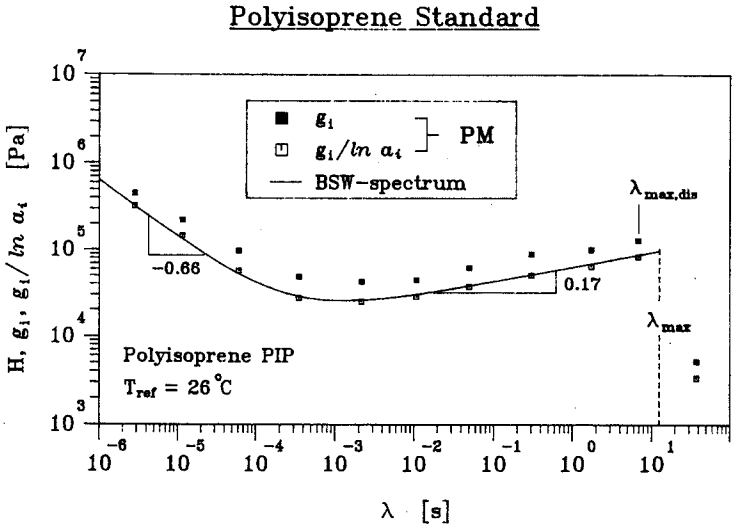


Fig. 9. Parallelism between the continuous BSW-spectrum and the discrete PM-spectrum. According to eqn. (14) the relaxation time ($\lambda$) of the discrete spectrum is shifted towards shorter times compared with the continuous BSW-spectrum.

pronounced with extremely wide spacing. Keeping in mind that the sample is not truly monodisperse, we also have to expect some weak modes with longer relaxation times.

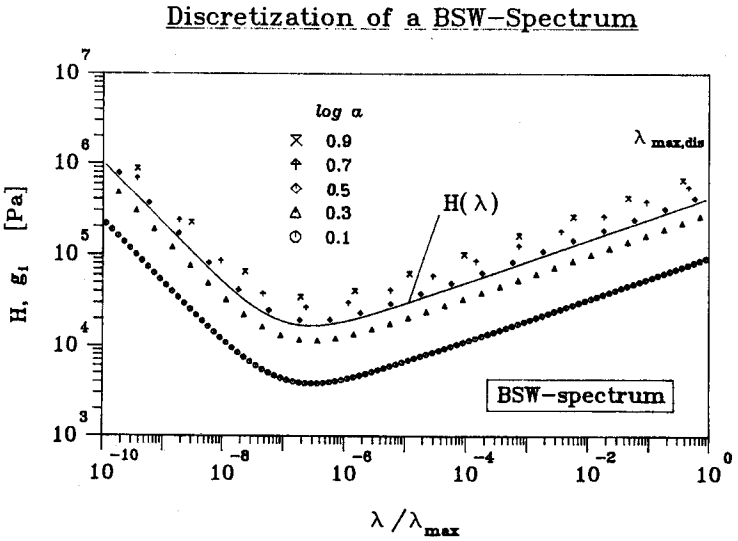


Fig. 10. A typical continuous BSW-spectrum is discretized. The longest relaxation time (cut-off time) is shifted towards shorter times depending on the spacing of the relaxation times. The spacing is varied from log $a$ = 0.1–0.9.

The leading relaxation time of the discrete spectrum (neglecting the weak Maxwell-mode due to broadening) is always shorter than the cut-off relaxation time $\lambda_{max}$. This affects the properties of the discrete spectrum, especially when modeling the terminal behavior. We shall study this shift in the cut-off relaxation time in the following analysis.

Following the procedure in the previous example (Section 3.1), a continuous BSW-spectrum is discretized (eqn. (10)) repeatedly with five different spacings (Fig. 10). We find that the leading relaxation time becomes shorter and shorter as the spacing increases

$$\frac{\lambda_{max.dis}}{\lambda_{max}} = \frac{1}{\sqrt{a}}. \tag{14}$$

We attribute this shift to our specific choice of discrete relaxation time which is approximately the geometric average of its corresponding time window in the continuous spectrum $[\lambda_{max}/a;\ \lambda_{max}]$; the geometric average for the boundary elements next to the cut-off becomes $\lambda_{max}/\sqrt{a}$ as used in the calculations.

In the entanglement regime, all curves of $G'$ and $G''$ which are calculated from the discrete spectra coincide with the dynamic data calculated from the continuous spectrum (Fig. 11). However, the transition to the terminal region is sharper if the spacing exceeds $\log a = 0.5$, and the terminal zone is affected.

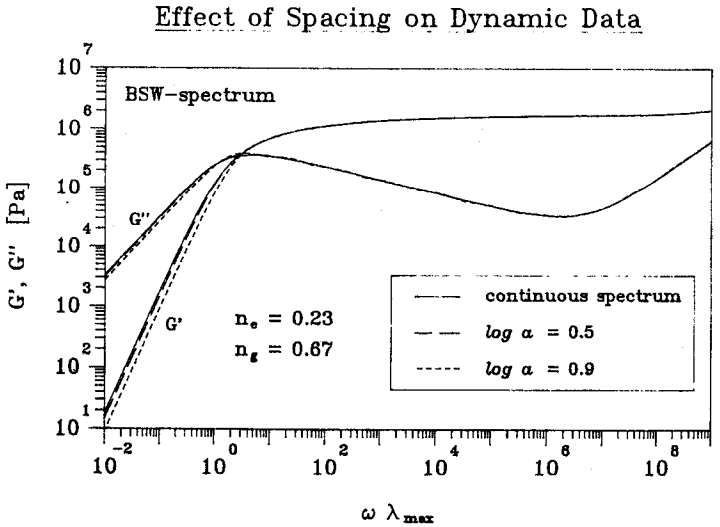


Fig. 11. The dynamic moduli which are calculated from the spectra in Fig. 10 have the same entanglement regime, while the transition to the terminal region is sharper for wide spacings.

## 4. Approximation of the continuous spectrum from discrete PM-spectra

The interconversion of the spectra will be demonstrated for the broadly distributed polymers. For that purpose, we consider a continuous spectrum $H(\lambda)$, express it in dynamic moduli $G'$, $G''$ and determine the PM-modes from this set of 'data'. The PM-modes are then converted into a continuous spectrum which should be identical with the initial $H(\lambda)$.

The relaxation times of discrete PM-spectra which are calculated from dynamic data are spaced non-equidistant. The order of magnitude of the spacing is about $\log a = 0.8$ which is fairly wide. Our objective is to investigate how closely the PM recovers the original spectrum. Due to the importance of this type of spectrum we also want to investigate the effect of noise in the dynamic input data on the calculation of such spectra. Additionally we would like to know how many data points per decade of frequency are appropriate for the spectra determination.

### *4.1 Effect of noise in the dynamic data on the parsimonious spectra*

We start out with the continuous spectrum of Fig. 4. The corresponding set of dynamic data $G'$, $G''$ is shown in Fig. 12 (solid lines). For the purposes of this study, artificial random noise is added to the dynamic data.

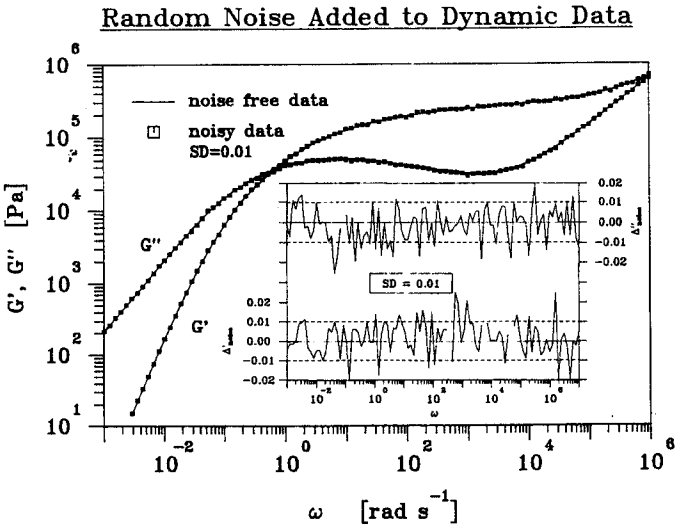


Fig. 12. Dynamic data from Fig. 5 with artificial random noise being added. The line through the points represents the noiseless data. In this example the standard deviation due to the noise is 0.01.

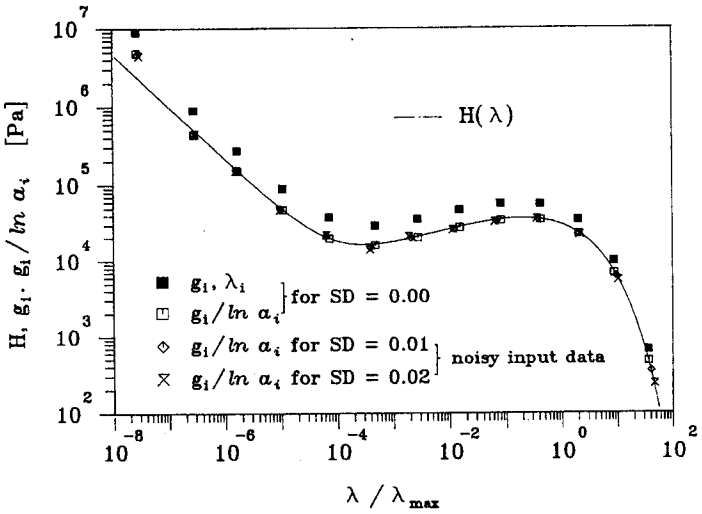


Fig. 13. Comparison of the calculated discrete spectrum with the original continuous spectrum in Fig. 4. Note that the recovery of the original spectrum is excellent. The deviation of the shortest relaxation mode is an artifact since the frequency window of the input data was limited from $\omega\lambda_{max} = 10^{-3}$ to $10^{7}$ which corresponds to a valid time window of the spectrum from $t_{min} = 10^{-7}$ to $t_{max} = 10^{3}$, $\lambda_{max}$.

The noise level which is characterized by the standard deviation, $SD_{noise}$, between the noisy data and the noise-free data

$$SD(G'')_{noise} = \sqrt{\frac{1}{M-1}\sum_{i=1}^{M}\left(\log G''_{i,noisy} - \log G''_{i,noise\text{-}free}\right)^2}, \tag{15}$$

is varied from $SD_{noise} = 0.0$ (noise-free data), $SD_{noise} = 0.01$ to $SD_{noise} = 0.02$. The discrete PM-spectra, as calculated from these 'data' and adjusted for the finite spacing (eqn. (9)), are plotted in Fig. 13. For reference, also plotted are the original relaxation modes, $g_i$, $\lambda_i$, of the noise-free data. Note that the spacing of the relaxation times is not equidistant. Therefore, the normalization-factor ln $a_i$, which shifts the discrete relaxation modes $g_i$ onto the curve of $H(\lambda)$, varies depending on the local spacing. The original spectrum is closely recovered by the PM even if the input data are unrealistically noisy. The small offset at the shortest relaxation mode is an expected artifact which is introduced by the cut-off at high frequencies in the dynamic data which were used to determine the spectrum.

This is a very encouraging result which shows that the discrete and the continuous forms of the spectrum are completely equivalent in their ability to describe the linear viscoelastic behavior. The algorithm is insensitive to the noise in the input data.

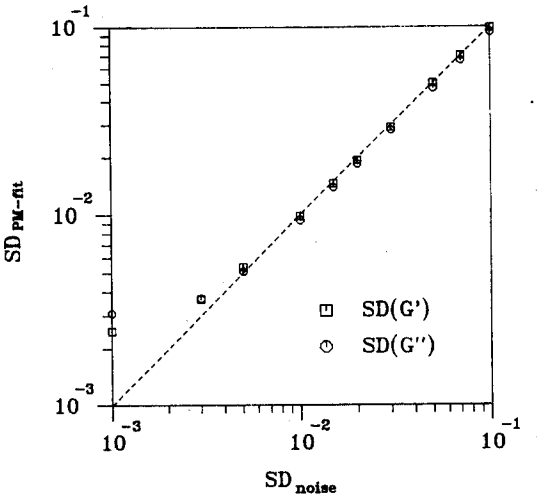


Fig. 14. Correlation between the standard deviation of the fit with the standard deviation of the noise added to the data. The simple one-to-one correlation allows a very good estimation of the scatter of the input data.

There seems to be a strong correlation between the closeness of the PM-fit and the noise of the data, as shown in Fig. 14. The standard deviation of the PM-fit

$$\mathrm{SD}_{\text{PM-fit}}(G'') = \sqrt{\frac{1}{M-1}\sum_{i=1}^{M}\left(\log G''_{i,\text{PM-fit}} - \log G''_{i,\text{noisy}}\right)^2} \tag{16}$$

is found to be proportional to the standard deviation due to noise, $\mathrm{SD}_{\text{noise}}$. Obviously, the SD of the fit cannot be significantly smaller than the SD of the noise of the dynamic input data. The simple one-to-one correlation allows us to estimate the noise level of experimental data from the standard deviation of the PM-fit.

### *4.2 Effect of data density on the determination of the PM-spectrum*

For the experimentalist it is very important to know the minimum number of dynamic data points per decade of frequency which is necessary to still be able to recover the original spectrum accurately. To find this lower limit of information, we proceed similarly as in Section 4.1. Noisy dynamic input data ($\mathrm{SD}_{\text{noise}} = 0.003$) are converted into PM-modes. The number of data points per decade of frequency (data density) is now varied in the range from 3 to 10. The resulting discrete spectra are shown in Fig. 15. Though the local spacing of the relaxation times depends somewhat on

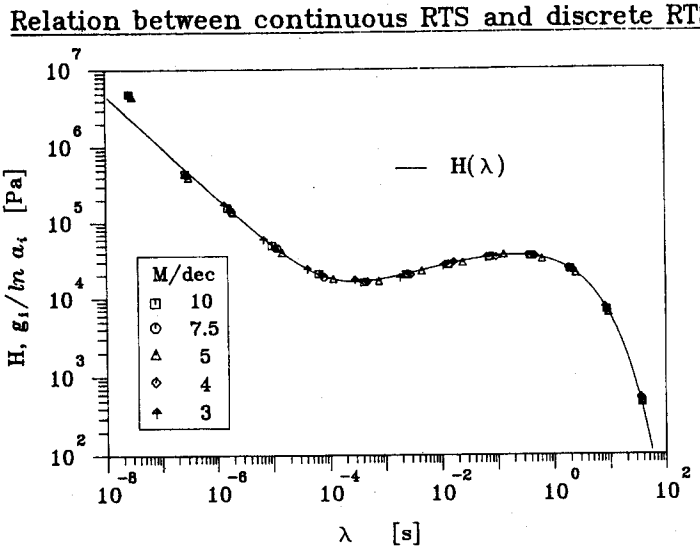


Fig. 15. The determination of the PM-spectrum is independent of the number of dynamic data points used as input.

the data sets, the continuous spectrum, $H(\lambda)$, is recovered in every case. Even a very low number (i.e. 3) of data points per decade is sufficient. However, from experience we recommend the use of at least 5 data points per decade of frequency to be on the safe side.

## 5. The parsimonious model (PM)

While working with relaxation spectra it became obvious that for every $G'$, $G''$ data set there exists an intermediate spacing (intermediate value for $N$ per decade)

$$N \text{ per decade} = 1/\log a \qquad \text{with} \qquad a = \sqrt[N]{\prod_{i=1}^{N} a_i} \tag{17}$$

at which the fitting is optimum [11]. Below that value, the spectrum is too wavy and, above this value, the pattern of the Maxwell-modes becomes erratic and inaccessible to analysis (ill-posed problem). This optimum discrete spectrum is the parsimonious model (PM) of the material. Knowing the parallelism between continuous and discrete spectra, we can now return to the PM and understand its origin.

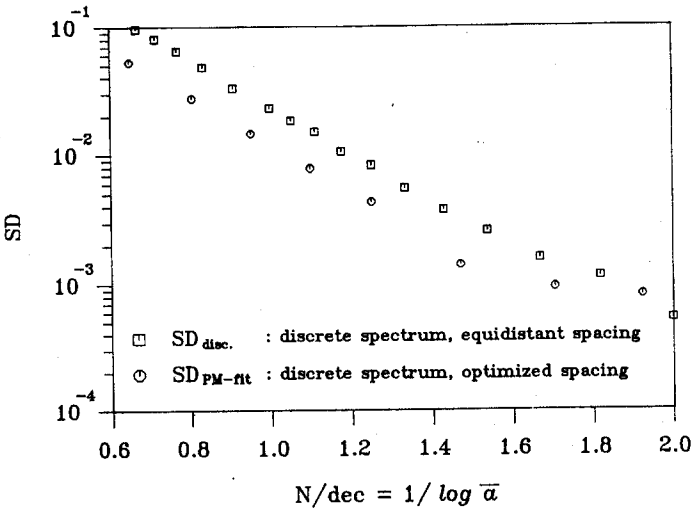


Fig. 16. A noiseless continuous spectrum is discretized (eqn. (11) with parameters of PP-2 of Fig. 2). The resulting standard deviation of the calculated $G'$, $G''$ curves with respect to the $G'$, $G''$ curves which are calculated from the continuous spectrum decreases with narrowing the spacing.

As a first step, we discretize a noiseless continuous spectrum (eqn. (11) with $\beta = 0.39$) and determine the resulting standard deviation,

$$\mathrm{SD}_{\mathrm{disc}}(G'') = \sqrt{\frac{1}{M-1}\sum_{i=1}^{M}(\log G''_{i,\mathrm{disc}} - \log G''_{i,\mathrm{cont}})^2} \tag{18}$$

in the loss modulus $G''$, and similarly for the storage modulus $G'$. The deviation decreases with narrowing of the spacing (Fig. 16). At wide spacings, the freely adjusting time constants give a somewhat better fit than the equidistant spacing, $a_i = \mathrm{const}$. The better fit is due to the fact that adjustable modes can shift to time scales where they are most needed. This

Fig. 17. (a) The standard deviation of the PM-fit of experimental data (i.e. polypropylene data, sample: PP-2) decreases with a closer spacing of modes. This improvement comes to a halt when the standard deviation of the fit reaches the noise level of the data. (b) All spectra calculated for the polypropylene sample PP-2 fall onto the same continuous spectrum, even if the spacing is extremely wide. The BSW-spectrum with stretched exponential cut-off at $\lambda'_{\max}$ is plotted for comparison (eqn. (11) with $\beta = 0.39$). (c) The local deviations between fit and $G'$, $G''$ data is shown for two of the discrete spectra of Figs. 17(a) and 17(b), a wide spacing with $N$ per decade = 0.7 and the optimum spacing with $N$ per decade = 1.2 (parsimonious spectrum). The deviations, $\Delta'$ and $\Delta''$, for the parsimonious spectrum are already dominated by the noise in the data.

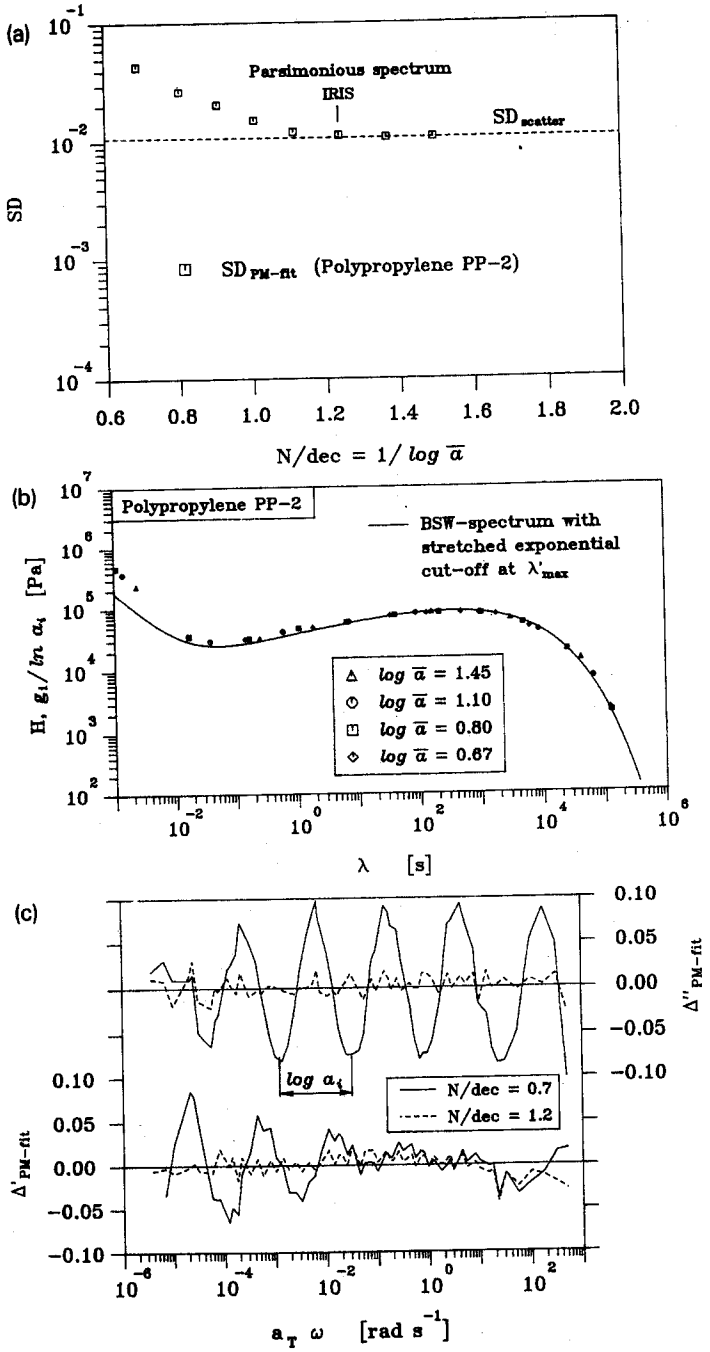
(a)
Parsimonious spectrum
IRIS
SD scatter
SD PM-fit (Polypropylene PP-2)
SD
N/dec = 1/ log ā
(b)
Polypropylene PP-2
BSW-spectrum with stretched exponential cut-off at λ'max
log ā = 1.45
log ā = 1.10
log ā = 0.80
log ā = 0.67
H, gi / ln ai [Pa]
λ [s]
(c)
log ai
N/dec = 0.7
N/dec = 1.2
Δ'PM-fit
Δ''PM-fit
aT ω [rad s-1]

bonus vanishes at very narrow spacing. There, the fit becomes equally good for adjustable and fixed $\lambda_i$, and the standard deviation continues to decay as the modes are placed closer and closer together. Such a result is completely expected when using a noiseless continuous spectrum as object to the modeling.

In the second step, we model real $G'$, $G''$ data of polypropylene PP-2. Again, the standard deviation decreases when placing the modes closer and closer together. This improvement comes to a halt when the standard deviation of the fit reaches the noise level of the data (Fig. 17(a)). Fortunately, this noise level is relatively low for many dynamical data sets and the calculated spacing of the relaxation modes is narrow enough to give a meaningful description of the intrinsic material time scales. The parsimonious model is found. Note that even for very widely spaced relaxation times, all modes fall onto the same continuous spectrum (Fig. 17(b)). The local deviations between fit and $G'$, $G''$ data are shown in Fig. 17(c) for two of the discrete spectra of Figs. 17(a)–17(b), a wide spacing with $N$ per decade = 0.7 and the optimum spacing with $N$ per decade = 1.2 (PM-spectrum). The deviations, $\Delta'$ and $\Delta''$, for the PM-spectrum are already dominated by the noise in the data.

A further narrowing of the spacing would result in a fitting of the data noise. The resulting Maxwell-modes would lose their material characteristic pattern and the procedure would become meaningless in this context, even if the standard deviation of the fit superficially improves. The problem can be circumvented by smoothing the data before discretization. Such smoothing is not addressed here, but the tools are available with the above conversion of discrete to continuous spectra. The danger of smoothing is that it introduces additional information which may lead to artifacts in the interpretation.

## 6. Conclusions

The relaxation-time spectrum of viscoelastic materials can be described interchangeably in the form of continuous or discrete spectra. The shape of a spectrum is not altered by the discretization, even if the spacing between neighboring relaxation times is not uniform. Comparing the discrete relaxation modes, $g_i$, $\lambda_i$, with the continuous spectrum, $H(\lambda)$, one observes that the relaxation strength of each discrete relaxation mode is shifted by a factor which depends on the local spacing of the relaxation times. For the case of spectra with sudden cut-off at $\lambda_{max}$, a shift of the leading (cut-off) relaxation time towards shorter times is observed due to the finite spacing. An additional weak Maxwell-mode (with $\lambda$ slightly above $\lambda_{max}$) has to be introduced for compensating this artifact.

All spectra of this study are truncated at short times. This introduces some errors at the short time limit of the spectra which will be analyzed in a separate study.

Material functions which are calculated from discrete spectra are slightly wavy. This waviness artifact is well below any practical importance if we use about 1.5 or more relaxation times per decade. The lower limit of the spacing between discrete modes is prescribed by the noise of the experimental data. From experience with wide ranges of $G'$, $G''$ data, this limit is given by 1.2–1.5 modes per decade, which is of the same order as the ideal spacing according to this study. More modes are not needed but, if attempted, they would require a smoothing of the data.

The calculation of the parsimonious spectrum is surprisingly insensitive to data noise or variations in data density. This property is unusual for a problem which is commonly recognized as being ill-posed. We conclude that the problem of converting G″, G″ data into a relaxation time spectrum is only very weakly ill-posed due to the deliberate choice of taking a small number of relaxation modes (parsimonious model). Increasing the number of modes would cause ill-posedness. This transition towards ill-posedness is outside the scope of this paper.

From a practical point of view, these findings are very encouraging, since they allow the reduction of continuous spectra to a small set of discrete relaxation modes as needed for model calculations and for material data bases.

## List of symbols

| | |
|---|---|
| $a$ | spacing between neighboring equidistantly spaced relaxation times |
| $a_i$ | spacing between neighboring relaxation times |
| $g_i$ | relaxation strength of discrete relaxation mode |
| $G(t)$ | relaxation modulus |
| $G_e$ | equilibrium modulus |
| $G'(\omega)$ | storage modulus |
| $G''(\omega)$ | loss modulus |
| $H(\lambda)$ | continuous relaxation time spectrum |
| $H(\lambda_i)$ | point on the continuous relaxation time spectrum |
| $J_e^0$ | recoverable compliance |
| $M$ | number of data points |
| $n_e$ | slope of BSW-spectrum in the entanglement regime |
| $n_g$ | slope of spectrum in the glass transition regime |
| $N$ | number of discrete relaxation modes |
| $SD_{PM\text{-}fit}$ | standard deviation between the PM-fit and the dynamic data set |
| $SD_{noise}$ | standard deviation between the noisy and the noise-free data set |
| t | time |

*Greek letters*

| | |
|---|---|
| $\delta(x)$ | delta function; $\delta(x=0)=1$ and $\delta(x\neq 0)=0$ |
| $\Delta$ | deviation between data point and calculated value |
| $\eta_0$ | zero shear viscosity |
| $\lambda$ | relaxation time |
| $\lambda_i$ | discrete relaxation time |
| $\lambda_{max}$ | longest (cut-off) relaxation time of the BSW-spectrum |
| $\lambda_{max,dis}$ | longest relaxation time of the discretized BSW-spectrum |
| $\lambda'_{max}$ | characteristic cut-off relaxation time of the BSW-spectrum with stretched exponential cut-off |
| $\lambda_i^-$ | right boundary of the relaxation time window |
| $\lambda_i^+$ | left boundary of the relaxation time window |
| $\omega$ | frequency |

**Acknowledgement**

This research was supported by the Materials Research Laboratory of the University of Massachusetts.

**References**

1 P.E. Rouse, J. Chem. Phys., 21 (1953) 1272.
2 P.G. de Gennes, Scaling Concepts in Polymer Physics, Cornell University Press, Ithaca, NY, 1979.
3 M. Doi and S.F. Edwards, The Theory of Polymer Physics, Clarendon Press, Oxford, 1986.
4 J.D. Ferry, Viscoelastic Properties of Polymers, Wiley, New York, 1980.
5 J.C. Maxwell, Philos. Trans., 157 (1866) 49.
6 F. Kohlrausch, Ann. Phys. Chem., 119 (1863) 337.
7 M. Baumgaertel, A. Schausberger and H.H. Winter, Rheol. Acta, 29 (1990) 400.
8 K. Ninomiya and J.D. Ferry, J. Colloid Sci., 14 (1959) 36.
9 R.I. Tanner, J. Appl. Polym. Sci., 12 (1968) 1649.
10 H.M. Laun, Rheol. Acta, 17 (1978) 1.
11 M. Baumgaertel and H.H. Winter, Rheol. Acta, 28 (1989) 511.
12 S.W. Provencher, Makromol. Chem., 180 (1979) 201.
13 G. Friedrich and B. Hoffmann, Rheol. Acta, 22 (1983) 425.
14 J. Honerkamp and J. Weese, Macromolecules, 22 (1989) 4372.
15 A.K. Livesey, P. Licinio and M. Delaye, J. Chem. Phys., 84 (1986) 5102.
16 C. Elster and J. Honerkamp, Macromolecules, 24 (1991) 310.
17 N. Orbey and M.D. Dealy, J. Rheol. 35 (6) (1991) 30.
18 G.H. Lindas, S.H. Dong, M.D. Rausch, Y.G. Lin, H.H. Winter and J.C.W. Chien, Macromolecules, 25 (1992) 1242.